Supplementary Information (SI) for Journal of Materials Chemistry A.

Supplementary information

A matter of design and coupling: High indoor charging efficiencies with organic solar modules direct coupled to a sodium ion battery

Li-Chung Kin *[ab], Andreas Distler [c], Oleksandr Astakhov [d], Bakary Kone [d], Hans Kungl [a], Andre Karl [a], Tsvetelina Merdzhanova*[d], Rüdiger-A. Eichel[ae], Christoph J. Brabec [cf], Uwe Rau [bdg]

[a.] *Institut für Energie- und Klimaforschung (IEK-9), Forschungszentrum Jülich GmbH, 52428 Jülich, Germany*
E-mail: l.kin@fz-juelich.de, t.merdzhanova@fz-juelich.de
[b.] *Faculty of Electrical Engineering and Information Technology, RWTH Aachen University, Mies-van-der-Rohe-Straße 15, 52074 Aachen, Germany*
[c.] *Institute Materials for Electronics and Energy Technology (i-MEET), Department of Material Science, Faculty of Engineering, Friedrich-Alexander-Universität Erlangen-Nürnberg, Martensstraße 7, 91058 Erlangen, Germany*
[d.] *Institut für Energie- und Klimaforschung (IEK-5), Forschungszentrum Jülich GmbH, 52428 Jülich, Germany*
[e.] *RWTH Aachen University, Mies-van-der-Rohe-Straße 15, 52074 Aachen, Germany*
[f.] *Helmholtz Institute Erlangen-Nürnberg for Renewable Energy (HI-ERN), Forschungszentrum Jülich GmbH, Immerwahrstraße 2, 91058 Erlangen, Germany*
[g.] *Jülich Aachen Research Alliance (JARA-Energy) and Faculty of Electrical Engineering and Information Technology, RWTH Aachen University, Schinkelstr. 2, 52062 Aachen, Germany.*

Spectral overlay of light source and OPV absorber layer

Spectrum overlay of AM1.5, 3000K LED and the EQE of the OPV module showing the good overlap between the spectrum of OPV module and that of the LED emission spectra. The high overlap of the EQE of the OPV module with that of an LED light source implies that there is no part of the spectrum that is lost to transmission, implying high efficiencies are possible.

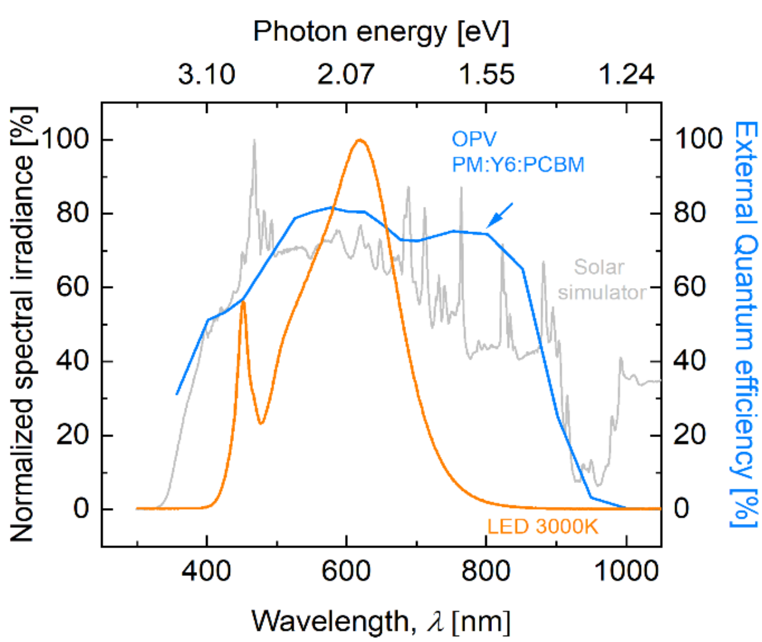

Figure S 1: Normalized spectral irradiance of a warm white (3000K) LED and solar simulator (AM1.5G) with external quantum efficiency of a PM6:Y6:PCBM organic solar cell

Summary of directly coupled PV-Battery performance

REF IN MAIN PAPER	AUTHOR NAME	DEVICE	OVERALL EFFICIENCY	PV EFFICIENCY	INTEGRATED/ DISCRETE	IRRADIANCE
1	Kin et al	PSC// NTP/Na	29.10%	43.90%	Discrete	24.5 $mWcm^{-2}$ LED
	This work	PM6:Y6 // NTP/Na	14.40%	15.61%	Discrete	5.212 $mWcm^{-2}$ LED
49	Li et al	III-V tandem //Flow battery	14.10%	26.10%	Integrated	1 sun
50	Hu et al	PSC module //Al/C	12.04%	18.50%	Integrated	1 sun
1	Kin et al	PSC module // NTP/Na	11.50%	12.20%	Discrete	1 sun
34	N. Agbo et al	a-Si:H /µc-Si:H//LTO/LFP	8.80%	9.20%	Discrete	1 sun
33	Sandbaumhüter et al	a-Si:H /µc-Si:H//Li/LCO	8%	8%	Discrete	1 sun
51	Xu et al	PSC series// LFP/LTO	7.80%	12.65%	Discrete	1 sun
52	Um et al	c-Si// LCO/LTO	7.61%	15.70%	Integrated	1 sun
53	Chen et al	C-PSC//Co_2P-CoP-$NiCoO_2$ /Zn	6.40%	11.10%	integrated	1 sun
54	Sun et al	DSSC fibre // $LiMn_2O_4$ / $Li_4Ti_5O_{12}$	Not reported	6.05%	Integrated	1 sun
56	Delgado Andrés et al	PBDB-T-2F / $PC_{60}BM$// P(PT-BT) / Li	1.60%	2.60%	integrated	1sun
58	Hoefler et al	PTB7-Th:O-IDTBR Tandem Cell // $Li_3V_2(PO_4)_3$ / VS_2	1.40%	5.00%	integrated	1sun
56	Andres et al	PBDB-T-2F / $PC_{60}BM$ // P(PT-BT) / Li	1.30%	2.60%	integrated	360 $mWcm^{-2}$ LED
55	Guo et al	DSSC TiO_2 nt //LCO/ TiO_2	0.82%	1.95%	Integrated	1 sun
58	Hoefler et al	PTB7-Th:O-IDTBR Tandem Cell // $Na_3V_2(PO_4)_3$ / $NaTi_2(PO_4)_3$	0.60%	5.00%	integrated	1 sun

Table S 1 summary of directly coupled PV-battery systems (without converter) under various states of integration and irradiance. Organic PV devices are highlighted in green. PSC=perovskite solar cells.

Table S1 contains the list of previously published papers featuring direct PV charging of a battery (without the use of power electronics), ranked by overall efficiency. The device in each publication is listed in the format: (PV//Battery cathode/Battery anode). PV efficiency is listed alongside the degree of integration (integrated device, or two discrete devices connected by wire) as well as the type and power of the irradiance used. From this table we can see that high PV efficiency does not always translate to a comparable overall efficiency; the direct connection of the PV device to a battery does not guarantee good performance of operation which can be related to suboptimal design. These design limitations may in many cases be attributed to the small scale of the test device and constraints concerning the number of PV and battery cells as well as the capacity of the lab scale batteries. Optimal design considerations are described in the dedicated section of the manuscript.

IV characterisation for the solar module under AM1.5 illumination

AM1.5	PCE [%]	FF [%]	P_{mpp} [mW]	V_{mpp} [V]	I_{mpp} [A]	V_{oc} [V]	I_{sc} [mA]	R_s [Ohm]	R_{sh} [Ohm]	Area [cm²]
5 cells	8.46	51.41	88.11	2.40	-36.71	3.63	47.22	25.24	1303.22	10.42
12 Cells	10.54	62.34	263.62	6.70	-39.35	8.89	47.59	29.85	5631.26	25

Table S 2 Characteristic properties of the solar module employed under AM1.5 illumination.

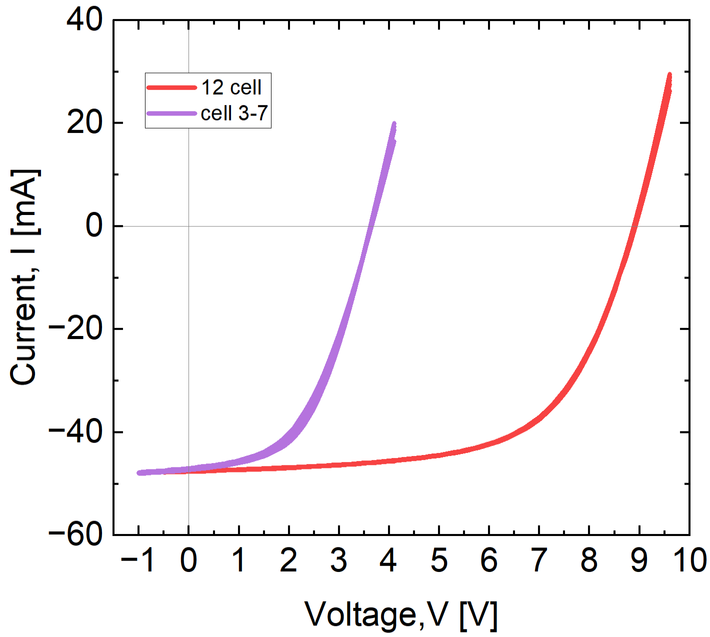

Figure S 2 IV characterization of the solar module under AM1.5 illumination.

The IV characteristics of the PV module are shown in figure S2 which was tested under AM1.5 conditions using a Sun simulator. The full module of 12 cells showed an efficiency of 10.54% and the 5 cells from 3-7 showed a power conversion efficiency of 8.46%.

The Wacom sun simulator is calibrated in house with eight world PV scale standard reference cells from ISE-Fraunhofer and checked weekly with two reference cells from PRC-Krochmann GmbH for homogeneity.

Circuit diagram and physical picture of the setup

Circuit diagram of the setup showing how the battery and the solar cell were connected to measurement equipment and switches. The resistor in the discharge circuit is in the switch box.

The solar module is attached to the setup via 4 crocodile clips and passes through the measurement box before connecting to the coin cell battery in the holder (figure S3, right). The whole setup is inside a darkened chamber that can be closed and isolated from outside light.

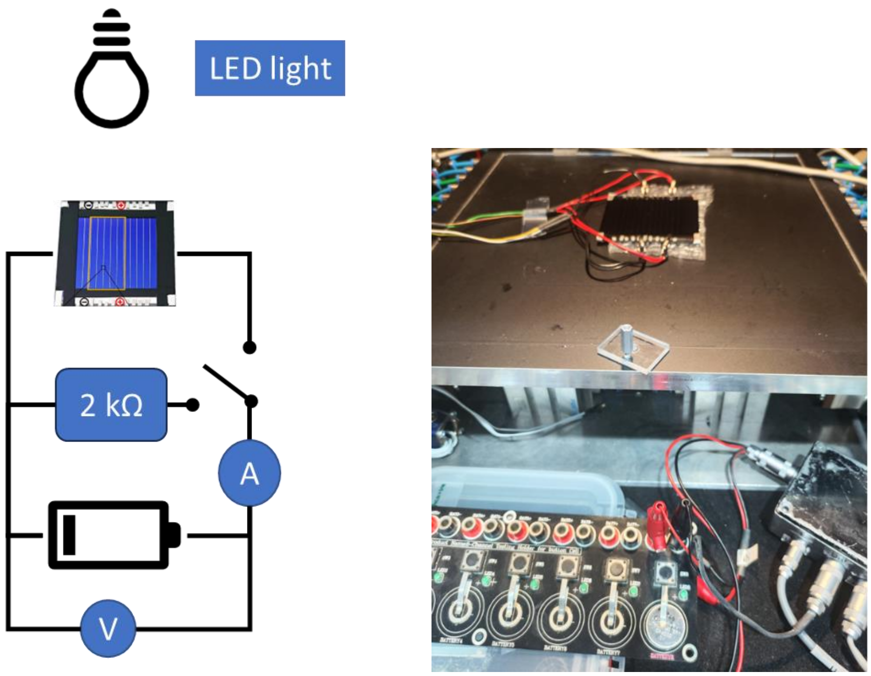

Figure S 3 Circuit diagram of the setup(left), with the picture of the setup and switch box on the right. The solar module is illuminated by the LED in the measurement chamber.

LED source characterization

LED Spectra

LED array spectra was measured and calibrated with a spectral analyzer for 150-15000 lx and can be seen here in figure S1 and normalized in figure S2. No obvious changes in spectra are seen apart from a slight blueshift of the spectra with increased intensity.

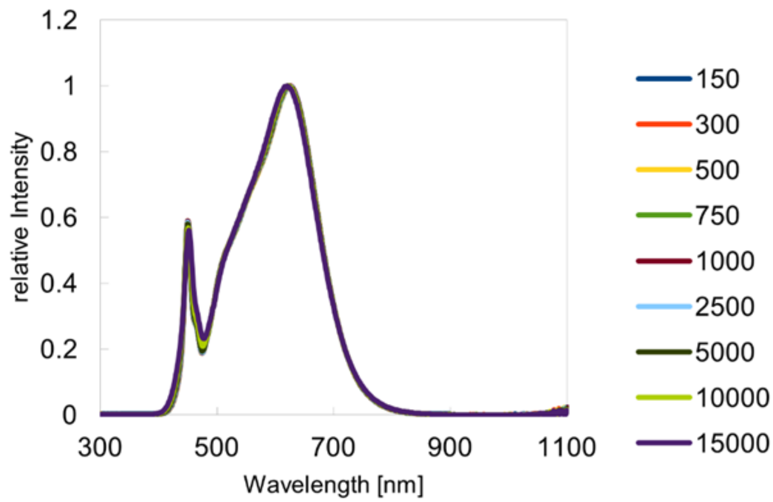

Figure S 4. Intensity spectra of the 3000 K LED source calibrated for lux values from 150 to 15000 lx

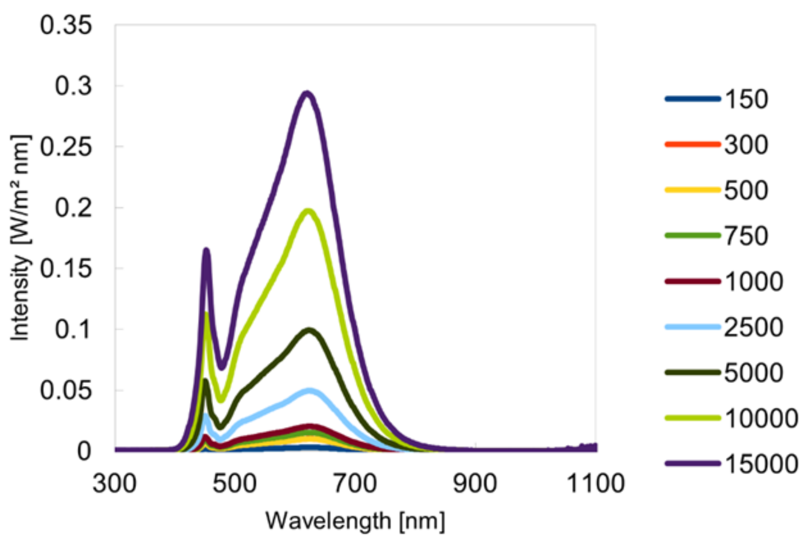

Figure S 5 Normalized Intensity spectra of the LED source calibrated for lux values from 150 to 15000 lx

Output stability curves for the LED array

Due to the temperature equilibrium that must be reached upon turning on the LED (figure S3 and S4), the decision was made to start from the lowest intensity and have at least a 150s between changes of intensity to allow for thermal equilibrium and not to turn off the LED array between measurements.

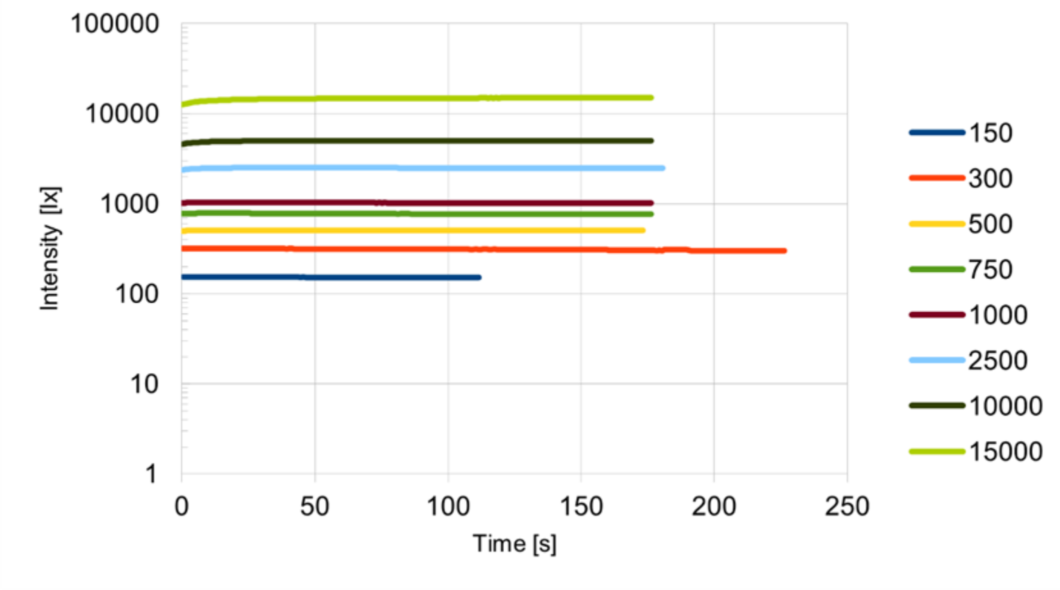

Figure S 6 Output intensity over time of the LED array from a cold start, in Lux

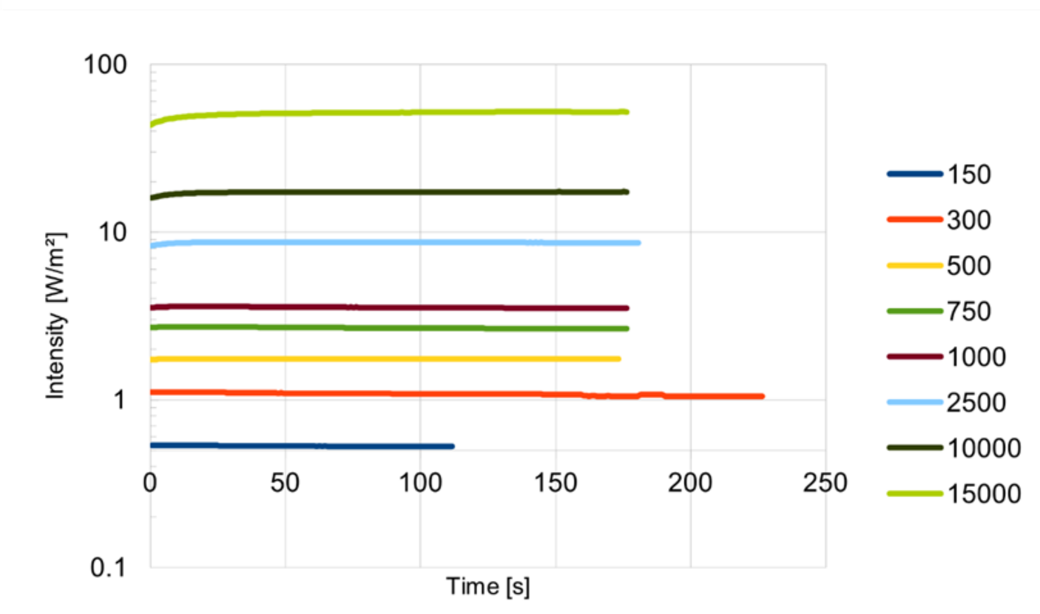

Figure S 7 Output intensity over time of the LED array from a cold start, in Wm^{-2}

Pictures of the system charging and powering a green LED

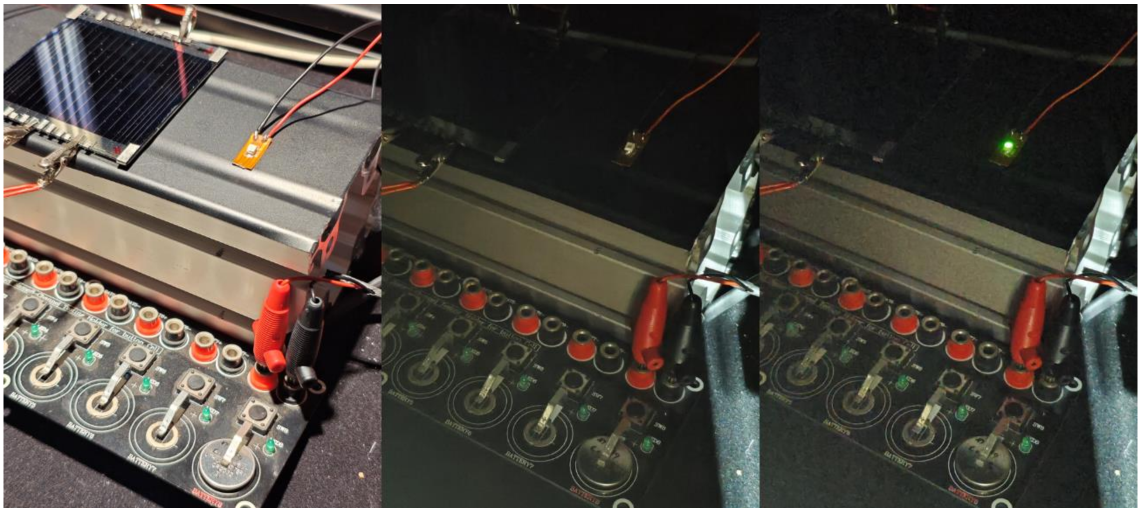

Figure S 8 (from left to right) the directly coupled PV-battery system charging under LED illumination, with the light source off and powering the green LED with the energy stored.

The battery is powerful enough to run a green LED with no control circuit directly and repeatedly. Charge-discharge cycle over the green LED was cycled thrice and drew a current of 0.03mA.

Definition of metrics

Coupling factor. The coupling factor [1, 2]

$$\boldsymbol{C} = \frac{\boldsymbol{P_{wp}}}{\boldsymbol{P_{mpp}}} \qquad \text{Equation 1}$$

of the system is the ratio of the output power of the PV at the working point (P_{wp}) with regards to the maximum possible PV power output (P_{mpp}) at each illumination intensity. A coupling factor close to 1 refers to how close the working point of the coupled system works with regards to the maximum power output of the PV module/cell and is important to maximize for high efficiency. High efficiency solar modules and batteries that are not paired properly to work at the correct voltage will have a low coupling factor and thus low efficiency. The working voltage of the directly coupled system is determined by the charging voltage of the battery and the working point can be visualized as the intersection of the current-voltage characteristics of both the battery and the solar module. [3]

PV charging efficiency. The efficiency of the PV module in charging the battery,

$$\eta_{PV-Batt}(\%) = \frac{V_c I_c}{A \times P_{light}} \qquad \text{Equation 2}$$

is a direct consequence of the coupling factor and is analogous to the solar-charging efficiency[1]. Here the charging voltage (V_c) and current (I_c) of the battery is divided by the effective area of the solar module (A) and the incident light power density upon the module (P_{light}). In this case it is either from the LED array (see SI for table of intensities to lux) or simulated sunlight (AM1.5G, 100 $mWcm^{-2}$).

It should also be noted that,

$$\eta_{PV-Batt}(\%) = \eta_{PV\ LED} \times C \qquad \text{Equation 3}$$

since,

$$\eta_{PV\ LED}(\%) = \frac{V_{mpp} I_{mpp}}{A \times P_{light}} \qquad \text{Equation 4}$$

Battery round trip efficiency. Battery round trip efficiency

$$\eta_{\text{round-trip}}(\%) = \frac{E_d}{E_c} = \frac{\int_{t_{d,start}}^{t_{d,end}} P_d \mathrm{d}t_d}{\int_{t_{c,start}}^{t_{c,end}} P_c \mathrm{d}t_c} \qquad \text{Equation 5}$$

refers to the fraction of energy stored for that cycle that can be extracted. E_d is the energy from the battery on discharge and E_c is the energy charged into the battery from the solar module. It is defined as the integral of the battery power curve during discharge (P_d) with respect to discharge time (t_d) over the integral of the battery power curve during charging ($P_c = I_c \times V_c$) with respect to the charging time (t_c).

Overall efficiency. The overall efficiency,

$$\eta_{\text{overall}}(\%) = \frac{E_d}{P_{light} \times A \times t_c} \times 100\%$$

$$= \frac{\int_{t_{d,start}}^{t_{d,end}} P_d \, \mathrm{d}t_d}{A \times (\int_{t_{c,start}}^{t_{c,end}} (P_{light}) \mathrm{d}t_c)} \times 100\% \qquad \text{Equation 6}$$

is the fraction of energy stored in the battery that can be extracted for that cycle charged by the PV module.[2] This is equivalent to the time integral of power discharged from the battery (P_d) over the incident light power on the solar module across the same time as a fraction of the time integral of incident light power (P_{light}) over the effective area (A) of the material .

It should also be noted that the overall efficiency,

$$\eta_{\mathrm{overall}}(\%) = \eta_{\mathrm{round-trip}} \times \eta_{\mathrm{PV-batt}} \qquad \text{Equation 7}$$

can also be expressed as a multiple of the battery round trip efficiency and the PV charging efficiency.

1. L. C. Kin, Z. F. Liu, O. Astakhov, S. N. Agbo, H. Tempel, S. C. Yu, H. Kungl, R. A. Eichel, U. Rau, T. Kirchartz and T. Merdzhanova, *Acs Applied Energy Materials*, 2020, **3**, 431-439.
2. L.-C. Kin, Z. Liu, O. Astakhov, S. Shcherbachenko, H. Kungl, T. Kirchartz, R.-A. Eichel, U. Rau and T. Merdzhanova, *Cell Reports Physical Science*, 2022, **3**, 101123.
3. O. Astakhov, T. Merdzhanova, L.-C. Kin and U. Rau, *Solar Energy*, 2020, **206**, 732-740.